



Research article

Effectiveness of the genus *Riccia* (Marchantiophyta: Ricciaceae) as a biofilter for particulate matter adsorption from air pollution

Winai Meesang¹, Erawan Baothong¹, Aphichat Srichat², Sawai Mattapha³, Wiwat Kaensa³, Pathomsorn Juthakanok⁴, Wipaporn Kitisriworaphan⁵, and Kanda Saosoong^{5,*}

¹ Green Space and Exercise Research Group, Department of Environmental Science, Faculty of Science, Udon Thani Rajabhat University, Udon Thani, 41000, Thailand

² Department of Mechanical Engineering, Faculty of Technology, Udon Thani Rajabhat University, Udon Thani, 41000, Thailand

³ Department of Biology, Faculty of Science, Udon Thani Rajabhat University, Udon Thani, 41000, Thailand

⁴ Center of Science and Technology for Research and Community Development, Udon Thani Rajabhat University, Udon Thani, 41000, Thailand

⁵ Natural Materials Research Group, Department of Chemistry, Faculty of Science, Udon Thani Rajabhat University, Udon Thani, 41000, Thailand

* **Correspondence:** Email: kanda.sa@udru.ac.th; Tel: +66862506204.

Abstract: The study of plants as a biofilter is highly relevant in the field of air pollution science to ecological restoration in urban, which is connected to the ecosystem and human health. The aim of this present study was designed to evaluate the use of *Riccia* as a biofilter for particulate matter. The treatment box was designed using the Computational Fluid Dynamic (CFD) model. The alignment of the biofilter plant was designed and performed in three different arrangements blocking, zigzag, and parallel panels. The particulate matter was generated by simulated B7 diesel fuel combustion smoke using a smoke generator and loaded into the chamber with air velocities of 0.5, 1.0, 1.5, and 2.0 m/s via a Laser dust sensor for both inlet and outlet air. The adsorption efficiency of the PM adsorbed on the biofilter plant was calculated. The physical properties, physiological, and biochemical parameters of the study plant such as Air pollution tolerance index (APTI), Dust capturing potential were investigated. Moreover, the micromorphological details of the plant, the volatile organic compounds (VOCs), polyaromatic hydrocarbons (PAHs), and adsorbed metal were analyzed. The study revealed adsorption efficiency was in the range of 2.3%–49.6 %. The highest efficiency values for PM₁, PM_{2.5},

and PM₁₀ were 31.4, 40.1, and 49.6, respectively, which belonged to the horizontal panel with a velocity of 2.0 m/s. The alignment of the panel and air velocities affects the efficiency. HS-GC-MS revealed that *Riccia* can be adsorbed the particulate matter and the quantity of Cd, Pb, and Na were 0.0044 ± 0.0069 mg/gDW, 0.0208 ± 0.0278 mg/gDW, and 0.9395 ± 0.1009 mg/gDW, respectively. The morphological study exhibited a rough surface to enhance the efficiency of the trapped particle matter. The results showed that *Riccia* was suitable for adsorbing the particulate matter with a diameter of 1–4 μm .

Keywords: particulate matter; liverwort; adsorption efficiency plants; APTI; dust capturing potential

1. Introduction

In recent decades, the rapid development of industry leads to high activities in commercial and agriculture causing an increase in the urban population. Consequently, the high utilization of natural resources leads to the emission of pollutants grew rapidly affect the air quality in the surrounding areas [1–4]. Almost all air pollutants such as nitrogen oxides (NO_x), sulfur oxides (SO_x), polycyclic aromatic hydrocarbons (PAHs), carbon monoxide (CO), volatile organic compounds (VOCs), and heavy metals come from road transport, which is generated by the combustion engines of the vehicles and other components such as brake and clutch linings and pads, tires, and fuel tanks. Moreover, particulate matter (PM) has been detected which is also formed in the atmosphere and is a major risk to human health [5]. Particulate matter has been classified by particle size as coarse (2.5–10 μm), fine (0.1–2.5 μm), and ultrafine (< 0.1 μm), also called nanoparticles because of their size restrict to the 100 nm or smaller particles. Their toxicity depends on the size of the particles because they are retained longer in the human body [6–8].

In recent years, many publications of the study on air pollution control have been published and various technologies have addressed the removal or reduction of toxic pollutants. There are different methods to treat the air pollutants such as the use of electrokinetic treatment [9], bioelectrochemical technology in the form of air-cathode single chamber microbial fuel cells (SC-MFCs) [10], nano-bioremediation technologies [11,12], bio-nanomaterials (nanofibrous air filters, nano-adsorptive materials) [13,14]. Nanotechnology's air pollution control system has been proposed in three categories: remediation and treatment, detection and sensing, and pollution prevention [15]. Even though the nanomaterials presented a high performance for air pollutant treatment, the synthesis of NMs is quite expensive and involves hazardous chemical substances. Therefore, phytoremediation technology has been established, the specific plants are employed to decontaminate the pollutants. The distinct plants accumulate pollutants in their parts and mobilize them into the tissues [16]. Phytoremediation is driven by solar energy, a natural method, and an inexpensive process; however, it is a long-term process.

Traditionally, air pollution assessment is based on monitoring of pollutants in the surrounding area and the analysis measurement related to chemical substances' effects on both the environment and organisms. The direct measurements of particulate matter have several techniques as measuring concentration (gravimetric, optical, and microbalance), size distribution Scanning Mobility Particle Sizer (SMPS), and Electrical Low-Pressure Impactor (ELPI) [17–19]. Therefore, plants are also used to be biomonitoring of air pollutants and are suitable tools for evaluating the levels of air pollutants,

having several advantages compared with the conventional methods [20,21]. Tree bark (e.g., black poplar tree, pine tree) is also used to examine the levels of toxic metals and trap the particulate matter in the atmosphere because their porous surface can enable efficient accumulation and retention of heavy metals [22–24]. The leaves of an ornamental tree (*Tibouchina granulosa* (Desr.) Cong.) with various types of trichomes located on the adaxial and abaxial surfaces have been investigated to adsorb particulate matter (PM) revealed that the adsorbed particles size range 2.5–100 μm and did not return to the environment under normal weather conditions [25].

Furthermore, lower plants like mosses and lichens can be used as atmospheric pollutant monitors. Lichens are used to be biomonitors of air pollutants such as particulate matter, Persistent Organic Pollutants (POPs), SO_2 , fluorides, ozone, nitrogen oxides, peroxyacetyl nitrate (PAN), and heavy metals due to their extraordinary capability to accumulate mineral elements and their occurrence at a large geographical range [26–29]. Mosses are effective in adsorbing and accumulating particulate matter (e.g., benzo(a)hexachloride isomers and polyaromatic hydrocarbons) in the air [30]. *Tillandsia usneoides* L. (Spanish moss) has been reported as a biomonitor assessing the particulate matter and examining particulate matter deposited on moss samples by SEM-EDS, ICP-MS, atomic absorption spectrometry [31], neutron activation analysis (NAA), etc. The Spanish moss grows in a zigzagging pattern, linear, twisted, and densely with scaled leaves, in addition, their trichomes include a stalk and flexible wings that can absorb water and nutrients directly from the air instead of their root, it does only adhere to a substratum. Consequently, Spanish moss is more effective to inhabit extreme conditions and is suitable for monitoring air pollution [32–34]. This method is inexpensive, easy to use, and is an alternative way to be developed on-site where there is no infrastructure or instruments for air quality monitoring. However, the adsorption and accumulation of the particulate matter probably depend on the morphology of the species due to the spaces between leaves and stems, so the focus should be on selecting plants for biomonitoring technology.

Poor air quality in Thailand is attributed to $\text{PM}_{2.5}$ which occurs from burned crop fields to harvest sugarcane or remove remnant biomass in the burning season, moreover, industries and vehicles are generated air pollutants [35]. Nevertheless, the research on mosses as biomonitoring is still low in numbers. Native thalli of the epiphytic lichen *Parmotrema tinctorum* were used as an effective tool for assessing metal pollutants in a Khao Yai Natural Park [36]. Thai native mosses have been reported as a bio-adsorbent to assess the heavy metal in the atmosphere [37]. However, the moss-containing building model used in particulate matter treatment had never been studied, just only the design of the air treatment plant provides only architectural aesthetics.

This study focuses on the use of *Riccia*, a genus of liverworts in the family Ricciaceae of division Marchantiophyta as biofilters in the adsorption chamber to treat the particulate matter. The alignment of plants used to treat air pollutants using flow dynamic mathematical models was performed using three different arrangements including blocking panels, zigzags panels, and parallel panels. The zigzag panels model revealed maximum absorption efficiency and were suitable for plant filters due to the high surface area to adsorb the air pollutants [38]. In this work, we built the absorption chamber to investigate the efficiency of *Riccia* for treating the particulate matter generated by a diesel smoke generator. Moreover, the second aim of this work was also to optimize the alignment of *Riccia* in the air chamber. The sample was identified based on morphological descriptions and taxonomic keys. The accumulated PM deposited on the thalli of *Riccia* was evaluated through SEM observations. We assumed that the development of bio-innovative research could help to solve and reduce urban air pollution.

2. Materials and methods

2.1. Materials and measurements

Glutaraldehyde, sodium cacodylate, and osmium tetroxide were used as received. Distilled water was used for plant sample preparation and washing purposes. The *Riccia* was obtained from the Moss Land shop, which is the online shop of the greenhouse garden in Nonthaburi Province in central Thailand. The species was identified by Assoc. Prof. Sahut Chantanaorrapint, Prince of Songkla University herbarium (PSU), Division of Biological Science, Faculty of Science, Prince of Songkla University, specializes in Bryophytes in Thailand. The ash content and moisture content were evaluated. The Air pollution tolerance index (APTI) which included four parameters; total chlorophyll, relative water content (RWC), Ascorbic acid content, and pH of extract plant was also measured. All samples were cut into similar pieces and had a dimension of $5 \times 5 \text{ cm}^2$. The study specimens were washed with deionized water and dried in the open air at room temperature. The absorption efficiency was performed in the treatment chamber with simulated diesel smoke. The concentration of particulate matter was measured with various airflow speeds of 0.5, 1.0, 1.5, and 2.0 m/s using the Laser dust sensor PMS3003 Arduino. Data were presented as mean values with standard deviation (SD). All graphs were produced with Origin 2021. In addition, the volatile organic compounds (VOCs) and polyaromatic hydrocarbons (PAHs) of the treated plant were analysed using Headspace gas chromatography/ mass spectroscopy (HS-GC-MS). The metals were analysed using Flame Atomic absorption spectroscopy (FAAS). A scanning electron microscopy (SEM) image was collected by the Hitachi S2500 scanning electron microscope to analyze the morphology of liverwort samples.

2.2. The selected plant in this research

In this research, the selected plant act as a biofilter is *Riccia* due to its morphology and ecology. *Riccia* is a genus of liverworts belonging to the Ricciaceae family of the Marchantiophyta division. It is complex thalloid liverworts that its thalli are internally differentiated. Its dorsal side tissue is green, while the ventral tissue side is colorless. The rhizoid walls are mostly densely papillose, with numerous papilla-like projections on the inner walls, and the ventral surface of the thallus is usually covered by multicellular scales, in two or more rows, which are often deeply purple. The reproduction can be either sexual or asexual. The genus *Riccia* is terrestrial, mostly growing on moist damp soil, rock, the bark of trees, and rotten wood, and adsorbs nutrients and water from the air through its outer surfaces instead of using roots, as many plants do [39]. It prefers moist habitats such as tropical montane cloud forests, moist damp soil, or shady places, and is used to be a good indicator of humidity because it can absorb large quantities of rainwater caused by thick layers of the thallus. In tropical cloud forests, the rainfall is captured by the liverworts up to 20%–40% [40]. It plays an important role in the water balance and nutrient cycles of the forest. Therefore, it has the possibility of the use *Riccia* as a biofilter. Recently, particular attention is focus on absorbing particulate matter from air pollution by living biomass such as mosses [41,42], and lichens [43].

2.3. Physical properties of the studied plant

2.3.1 Ash content

The ash content is used to determine the total composition of biomass samples, which consists of the mineral content and other inorganic matter in biomass. The sample was weighed 0.5 g, to the nearest 0.1 mg of a test specimen into the tared crucible which was prepared by placing them in the furnace at 600 °C for a minimum of three hours and allowed to cool at room temperature in a desiccator. Place the sample into the furnace at 600 °C for a minimum of three hours and dry to constant weight. Constant weight is defined as less than ± 0.3 mg change in the weight upon one hour of re-heating the crucible. The ash content was calculated by using Eq (1) as follows:

$$\text{Ash content (\%)} = \frac{W_{CA} - W_C}{W_i} \times 100, \quad (1)$$

where W_{CA} , W_C , and W_i are the weight of the crucible plus ash, the weight of the crucible, and the dry weight of the sample, respectively.

2.3.2 Moisture content

The measurement of moisture content by direct measurement is determined by removing moisture in an oven and then by measuring weight loss. The sample was weighed 0.5 g, to the nearest 0.1 mg of a test specimen into the beaker which was prepared by placing them in the oven at 105 °C for a minimum of six hours and allowed to cool in a desiccator. Place the sample into the oven at 105 °C for a minimum of six hours and dry to constant weight. Constant weight is defined as less than ± 0.3 mg change in the weight upon one hour of re-heating the beaker. The moisture content was calculated by using Eq (2) as follows:

$$\text{Moisture content (\%)} = \frac{W_i - W_t}{W_i} \times 100, \quad (2)$$

where W_i and W_t are the initial weight of the plant, and the terminated weight of the plant, respectively.

2.4. Measurement of physiological and biochemical parameters

2.4.1. Relative water content (RWC)

1.0 g of the study plant (fresh weight; FW) was floated in distilled water in darkness at 4 °C for 24 h. Then, dried with filter paper and its turgidity weight (TW) was determined. Place it into the oven at 70 °C for 24 h to determine its dry weight [44]. RWC was calculated by using Eq (3) as follows:

$$\text{RWC} = \frac{[\text{FW}-\text{DW}]}{[\text{TW}-\text{DW}]} \times 100. \quad (3)$$

2.4.2. Plant extract pH

1.0 g of the study plant was crushed by porcelain mortar and homogenized in 10 mL of deionized distilled water. The sample was centrifuged at 2,400 rpm for 10 min and the pH was measured using a pH meter.

2.4.3. Total chlorophyll content (TCH)

1.0 g of the study plant was crushed and 10 mL of 80% acetone was added. Allow to room temperature for 15 min for thorough extraction. The extract was centrifuged at 2,400 rpm for 10 min. Then, the absorbance was measured at 645 nm and 663 nm using a spectrophotometer after calibrating with the reagent blank. The chlorophyll A, chlorophyll B, and total chlorophyll content were calculated using Eqs (4)–(6) as follows [45]:

$$\text{Chlorophyll A} = [12.72 (A_{663}) - 2.69 (A_{645})] \times \left[\frac{V}{1,000W} \right], \quad (4)$$

$$\text{Chlorophyll B} = [22.9 (A_{645}) - 4.68 (A_{663})] \times \left[\frac{V}{1,000W} \right], \quad (5)$$

$$\text{Total chlorophyll} = [20.2 (A_{645}) + 8.02 (A_{663})] \times \left[\frac{V}{1,000W} \right], \quad (6)$$

where A_{645} , A_{663} , V , and W are the absorbance at 645 nm, absorbance at 663 nm, the total volume of the extract (mL), and the weight of the sample (g), respectively.

2.4.4. Ascorbic acid (AA)

The ascorbic acid content was measured by the method of titration with 2,6-dichlorophenol indophenol (DCIP). 1.0 g of the study plant was homogenized by grinding in a pestle with a mortar and 5% oxalic acid was added to avoid such a loss of ascorbic acid. The extract was filtered, and the volume is made up to 100 mL with 5% oxalic acid. Then, 10 mL of the unknown solution was titrated with the DCIP dye, and the appearance of pink color indicated the endpoint. 10 mL of ascorbic acid solution and 5% oxalic acid were titrated with DCIP dye for standard and blank solutions. The ascorbic acid content was calculated by using Eq (7) as follows:

$$\text{Ascorbic acid} = \left[\frac{U-B}{S-B} \right] \times \frac{\text{A total volume of unknown}}{\text{The volume has taken for each sample}} \times \text{Amount of AA in 10 mL of standard}, \quad (7)$$

where U , S , and B are the titre value of unknown, titre value of standard, and titre value of blank, respectively.

2.4.5. Air pollution tolerance index (APTI)

APTI of the plant was measured by four parameters of RWC, pH, TCH, and AA using Eq (8) as

follows:

$$\text{APTI} = \frac{[A(T+P) + (R)]}{10}, \quad (8)$$

where A, T, P, and R are ascorbic acid content (mg/g of dry weight), total chlorophyll content (mg/g), plant extract pH, and relative water content (%), respectively.

APTI values were categorized into four tolerance levels, there are level (1) tolerant (T) species, level (2) moderately tolerant (MT) species, level (3) intermediate (I) species, and level (4) sensitive (S) species [45].

2.4.6. Dust capturing potential

Three replicates of plant specimens were cut into similar pieces with the dimension of 1×1 cm and transferred to the zip bag which was weight before use. The dust was generated from talcum powder and the particle size was measured using the Laser dust sensor PMS3003 Arduino. The sizes ranged from 1.0–30.0 μm . The dust was added to the zip bag and the weight of the plant with dust and zip lock bag was measured. Then, the dust was removed and the weight of the plant after removing of dust was determined. The dust-capturing potential of the plant was calculated using Eq (9) as follows:

$$W = \frac{(W_1 - W_2 - W_3)}{A}, \quad (9)$$

where W, W_1 , W_2 , W_3 , and A are dust-capturing potential (g/cm^2), the weight of plant with dust and zip lock bag (g), the weight of plant after removing dust (g), weight of zip lock bag (g), and total area of the plant (cm^2).

2.5. Particulate matter

The particulate matter used in the experiment was generated by simulated fuel combustion smoke using a diesel smoke generator and loaded into the tank with a capacity of 200 liters by a fan. The generated particulate matter was distributed by the size ranges (in micrometers) as follows: PM1, PM2.5, and PM10. The concentration was set at $5,000 \pm 250 \mu\text{g}/\text{m}^3$ using automatic adjustment of the smoke pipe valve from the controlled program. The smoke was released into the adsorption chamber through a 1-meter-long pipe via the PM2.5 concentration sensor (Laser dust sensor PMS3003 Arduino) with the flow speed of air pollutants at the inlet of the box of 0.5, 1.0, 1.5, and 2.0 m/s.

2.6. The study of adsorption efficiency

All plant samples were prepared in the open-air room and cut into a similar pieces with an area of $5 \times 5 \text{ cm}^2$. The adsorption efficiency of the PM adsorbed on the biofilter with the various wind speed conditions was measured. The inflow air velocity was set to four different velocities of 0.5, 1.0, 1.5, and 2.0 m/s for one hour each. The initial concentration of PM2.5 and the remaining PM2.5 were measured before and after entering the treatment box, respectively. Four panels set up the chamber with the different alignments of sample plants, vertical, zigzag, and horizontal. Each panel has three points in a vertical line and four points in a horizontal line and the distance from each other is 10

centimeters, therefore, there are twelve points of each panel in the treatment box as described by Meesang et al. [38]. The control system measured the concentration of PM_{2.5} before entering and after entering through the adsorbed plants in the treatment box. All data were selected using IBM SPSS statistics 25 followed by Microsoft excel for calculating the adsorption efficiency value. The scattering graphs were plotted using Origin 2021. The adsorption efficiency was expressed as a percentage of the residue matter compared to its initial concentration by using Eq (9) as follows [46]:

$$\eta (\%) = \left[\frac{\text{PM}_{2.5\text{IN}} - \text{PM}_{2.5\text{OUT}}}{\text{PM}_{2.5\text{IN}}} \right] \times 100, \quad (9)$$

where PM_{2.5IN} and PM_{2.5OUT} are the initial and remaining concentrations of a particulate matter 2.5, respectively.

2.7. Determination of VOCs and PAHs by using HS-GC-MS

The indirect determination of volatile organic compounds (VOCs) and polyaromatic hydrocarbons (PAHs) constituents in plant samples by analysing the vapor phase that is in thermodynamic equilibrium with the sample in a closed system using headspace gas chromatography/mass spectroscopy (HS-GC-MS). The extraction was performed in an HS vial filled with plant samples and sealed with a silicone septum cap, thermostated for 15 min at 105 °C. Once equilibrium between the matrix and the gaseous phase was reached, the HS needle descended, pierced the septum cap, and pressurized with nitrogen at 45 psi for 3 min. Then, the over-pressured gas sample in the HS vial was applied to the GC column at 120 °C with a flow rate of 1 mL/min. Subsequently, the GC column was used to separate the VOCs and PAHs. The mass spectrometer was used as the detector. The data was carried out for 14 min at a scan rate of 1 scan s⁻¹. Peak identification in the HS-GC-MS chromatograms was done by comparing their mass spectra with those contained in the NIST (National Institute of Standards and Technology) library.

2.8. Determination of metal by using FAAS

For analysis of the samples with atomic absorption spectrophotometry, plant samples of around 0.5 g were digested in a solution of HNO₃:H₂O₂ (7:2) in Teflon digestion vessels and exposed to microwaves (METASH, MWD-610). The digestion was carried out in 2 steps, in the first step, the solution was heated at 180 °C for 20 min ramp time, and the next step was carried out at 180 °C for 20 min hold time with a power of 800 W. Finally, the vessels were allowed to cool and carefully opened, the digest solution transferred into 50 mL of volumetric flask and volume adjusted by added the distilled water. Metal concentrations were measured by atomic absorption spectrophotometry (Perkin-Elmer, PinAAcle 900F). Samples were analyzed in triplicates and the results were given in mg/g dry weight.

2.9. Morphology of plant

All plant samples were cut into pieces, approximately 4 mm long, and immediately fixed in glutaraldehyde (2.5%) in sodium cacodylate buffer (0.1 M, pH 7.2–7.4) at 4 °C for 4 hours, rinsed three times in sodium cacodylate / Phosphate buffer (pH 7.2–7.4) at 4 °C for 15 minutes each. Post-

fixed sample with 1.0% Osmium tetroxide in buffer at 4 °C for 1 hour. Dehydrated tissue with a series of ethanol from 30% v/v-100% v/v ethanol at 4 °C, 2 times for 15 minutes each. Dried by the CO₂ critical point (Hitachi HCP-2), the samples were mounted on stubs with double-coated conductive carbon tape. Then samples were coated with Pt-Pd for 4 minutes in Hitachi E-102 ion sputter. The plants were observed and photographed with Hitachi S2500 Scanning Electron Microscope. The size distribution curve of particles adsorbed on the sample plant was measured and analyzed by ImageJ software [47]. The scale bar of each image was used to calibrate the software before particle measurements. All particles size were obtained from a mean value of two values equivalent to the orthogonal axes in micrometers unit.

3. Results and discussion

3.1. Physical properties of plant

The ash content and moisture content were 14.44 ± 1.54 and 6.32 ± 0.34 , respectively. The results revealed that the lower the dry matter the higher the ash due to the moisture content affecting the initial weight of the sample as shown in Table 1. Owing to the ash content is the amount of inorganic noncombustible material, which is residues after a completely burnt, such as oxides of the inorganic elements including metal salts which are important for photosynthesis processes requiring ions such as Na⁺ (Sodium), K⁺ (Potassium), and Ca²⁺ (Calcium) [48], and trace minerals which are required for unique molecules, such as chlorophyll and hemoglobin [49]. The obtained value (14.44%) shows a higher as compared to Spanish mosses (3.7%–7.0%) [50]. It means *Riccia* can be absorbed some minerals or trace elements and are essential for many processes. Moreover, the plants may have a short or long shelf life depending on the moisture content. The plant saps reflect the ability of a plant to exist under widely different environmental conditions, and the ability to adjust its tissue fluids to the new environment [51]. *Riccia* has a higher moisture content as compared to some plants such as *Rauvolfia serpentina* (0.73%) [52] and *Sphagnum* spp. (0.70%) [53]. From the above mentioned, *Riccia* has the potential to absorb the particulate matter and has a high tolerance to the stress condition.

Table 1. The ash content and moisture content.

| Parameter | Value |
|------------------|------------------|
| Ash content | 14.44 ± 1.54 |
| Moisture content | 6.32 ± 0.34 |

3.2. Physiological and biochemical properties of plant

3.2.1. Air pollution tolerance index (APTI)

The RWC showed a high value of $87.32 \pm 4.15\%$, which RWC referred to the current water content of the leaf tissue relative to the full turgid water content, normally RWC in leaves ranges between 98%, in turgid and transpiring leaves to around 20%–50%, and RWC at initial wilting is about 60% to 70% [54]. The high level of relative water content leads to a high tolerance ability to air pollutants owing to high RWC to retain its physiological balance and prevent the loss of water and nutrients [55]. The pH of an extracted plant is neutral with a value of 7.2 ± 0.1 . Plants with a low pH

showed high sensitivity to air pollutants, especially SO₂ and NO₂. Their stomata were faster closed when exposed to air pollutants [31]. pH adjustment plays an important role in the movement of vesicles and intracellular compounds. When plants are exposed to air pollutants (especially SO₂), large amounts of H⁺ are produced in the intercellular fluid to react with SO₂, therefore this H⁺ may produce H₂SO₄, leading to decreased pH of the leaf extract. *Riccia* exhibited a low chlorophyll concentration of 0.1542 ± 0.0124 mg/g fr wt. Air pollution has a great influence on the total chlorophyll of plants because the photosynthetic pigment has been degraded when exposed to air pollutants. Therefore, the total chlorophyll of plants decreases as air pollution increases. Ascorbic acid content was found less with a value of 0.74 ± 0.11 mg/g fr wt. Ascorbic acid revealed a strong reducer and plays a role in photosynthetic carbon fixation, cell wall synthesis, defence system, and cell division. The antioxidant capacity of ascorbic acid affects its resistance to air pollution. Plant with a low ascorbic acid content has a high sensitivity to air pollution. In the study, all four parameters can be calculated the APTI value which indicated that *Riccia* showed a sensitive level to air pollutants with a value of 9.27. It can be used as a bioindicator of air pollution. Physiological and biochemical properties are presented in Table 2.

Table 2. Physiological and biochemical properties.

| Parameter | Value |
|--------------------------------------|---------------------------------|
| Relative water content (RWC) | $87.32 \pm 4.15\%$ |
| Plant extract pH | 7.2 ± 0.1 |
| Total chlorophyll content (TCH) | 0.1542 ± 0.0124 mg/g fr wt. |
| Chlorophyll A | 0.1142 ± 0.0090 mg/g fr wt. |
| Chlorophyll B | 0.0400 ± 0.0034 mg/g fr wt. |
| Ascorbic acid (AA) | 0.74 ± 0.11 mg/g fr wt. |
| Air pollution tolerance index (APTI) | 9.27 |

3.2.2. Dust capturing potential

Dust collecting capacity of plants depends on their morphological traits like phyllotaxy, leaf shape, size and texture, presence or absence of hairs, stomatal frequency, surface roughness, stomatal density, and trichome length. The median dust-capturing potential of *Riccia* has a higher value of 0.0667 ± 0.0172 g/cm² (Table 3) as compared to greening plant species (0.387 – 0.451 g/cm²) [56]. The *Riccia* revealed dust-capturing potential to reduce particulate matter, therefore it acts as a biological air filter.

Table 3. Dust capturing potential.

| Dust capturing potential | Value |
|--------------------------|---------------------------------------|
| Median | 0.0667 ± 0.0172 g/cm ² |
| Interquartile range, IQR | 0.0121 |

3.3. Adsorption efficiency

The adsorption efficiency of *Riccia* with four different velocities of 0.5, 1.0, 1.5, and 2.0 m/s was

in the range of 2.3%–49.6% as shown in Table 4. The highest efficiency values for PM1, PM2.5, and PM10 were 31.4, 40.1, and 49.6, respectively, which belonged to the horizontal panel with a velocity of 2.0 m/s. As compared to the previous results from *Epipremnum aureum* with the removal efficiencies of 75.2% for PM2.5, and 71.9% for PM10 [57] and *Tillandsia usneoides* exhibited the removal efficiency of 16.5% for PM2.5 from incense and 9.2% for A1 rigid, respectively [58]. From our previous work [38], the CFD calculation shows the optimum condition for trapped particulate matter was alternating zigzags panels due to the air pollution in all air inlets that can be contacted with the surface area of the study plant at all twelve positions. On the other hand, the results show that the horizontal panel has the highest values might be from the air circulation has no blocking from the panel, while the zigzags have partially blocked. Owing a higher airflow rate creates turbulent conditions in the treatment box, in which the motion particles display transverse motion, all particles oscillate along paths at right angles to the direction of the wave's advance, and as a result, all 12 points of the sample plant in the horizontal panel were contacted with the particulate matter leading to high adsorption capacity [59,60]. It can be concluded that the alignment of the panel affects the efficiency. Moreover, the air velocities affect the adsorption efficiency. Figure 1 demonstrates the effect of different air velocities on the adsorption efficiency which showed that the increased velocity increased the efficiency. Generally, higher velocities in the gas phase refer to the diffusion rates being higher leading to a shorter residence time, however, the results showed that the increased air velocities increased adsorption efficiency because high airflow velocity causes airflow turbulence and generates transverse motion which enhances the rate of energy and momentum exchange increasing heat transfer and friction coefficient leading to gas-solid mass transfer [61]. As a result, air circulation around the treatment box contributes to mass transfer between air pollutants and the study plant at all positions affecting the higher dust absorption.

Table 4. The adsorption efficiency with four different velocities of 0.5, 1.0, 1.5, and 2.0 m/s.

| Air velocity (m/s) | Panel alignment | Adsorption efficiency (%) | | |
|--------------------|-----------------|---------------------------|-------------|-------------|
| | | PM1 | PM2.5 | PM10 |
| 0.5 | Vertical | 2.3 ± 4.8 | 24.4 ± 1.7 | 29.6 ± 3.0 |
| | Zigzag | 3.3 ± 4.4 | 3.7 ± 2.0 | 7.1 ± 5.9 |
| | Horizontal | 16.6 ± 3.7 | 31.5 ± 12.6 | 15.5 ± 4.7 |
| 1.0 | Vertical | 7.3 ± 3.6 | 14.9 ± 7.2 | 30.2 ± 4.3 |
| | Zigzag | 15.6 ± 3.3 | 26.5 ± 6.9 | 36.2 ± 4.6 |
| | Horizontal | 12.5 ± 5.6 | 22.3 ± 10.3 | 39.9 ± 6.2 |
| 1.5 | Vertical | 19.6 ± 4.9 | 21.3 ± 6.0 | 23.6 ± 5.2 |
| | Zigzag | 3.3 ± 3.5 | 6.1 ± 3.1 | 18.6 ± 2.6 |
| | Horizontal | 11.0 ± 10.5 | 29.0 ± 12.7 | 40.3 ± 14.9 |
| 2.0 | Vertical | 12.0 ± 4.7 | 21.8 ± 9.0 | 25.8 ± 1.7 |
| | Zigzag | 12.6 ± 4.0 | 15.9 ± 1.6 | 36.2 ± 4.5 |
| | Horizontal | 31.4 ± 5.2 | 40.1 ± 10.8 | 49.6 ± 9.6 |

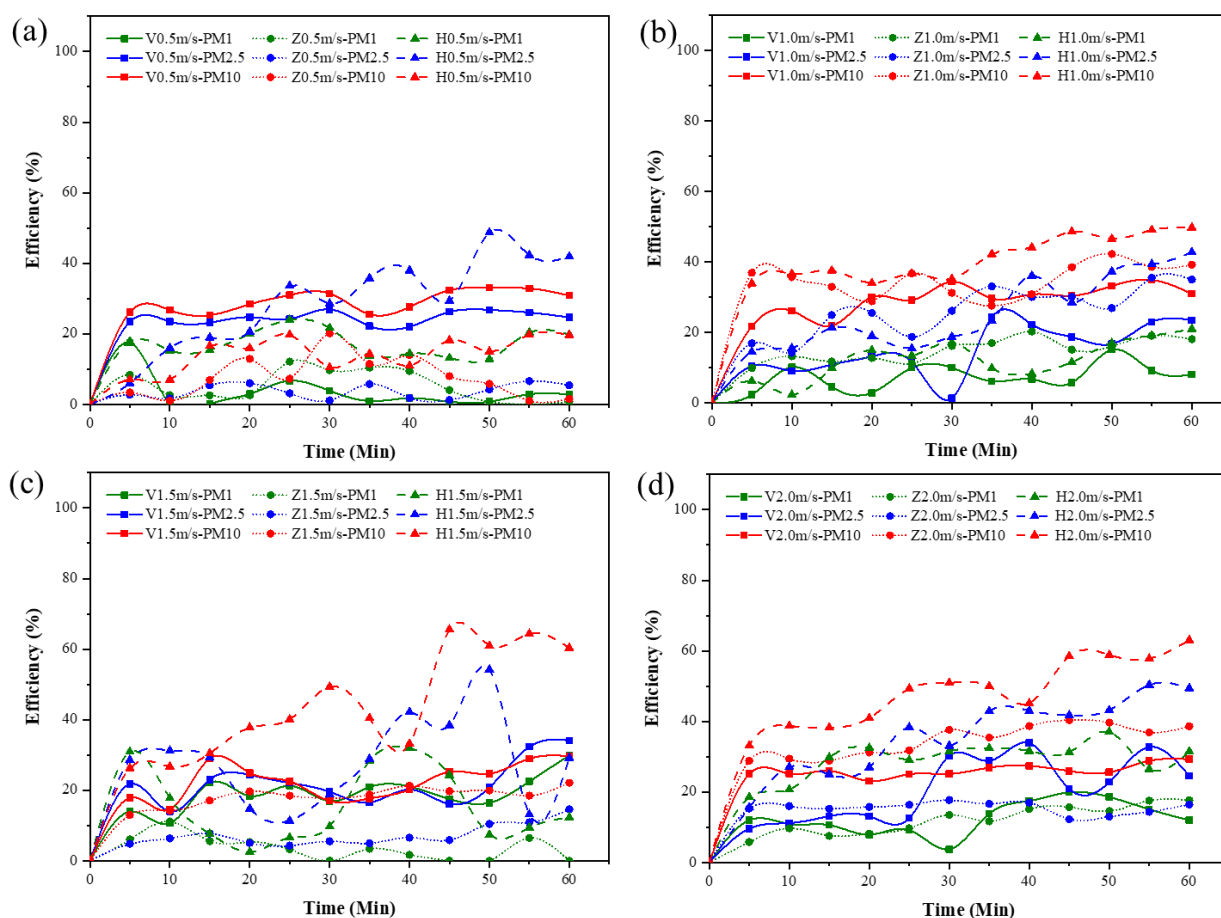


Figure 1. The absorption efficiency of *Riccia* for capturing PM1, PM2.5, and PM10 using vertical, zigzag, and horizontal airflow patterns at a velocity of (a) 0.5, (b) 1.0, (c) 1.5, and (d) 2.0 m/s.

3.4. VOCs and PAHs analysis

The chromatogram of the particulate matter treated and untreated *Riccia* was displayed in Figure 2. The chromatogram of the particulate matter treated shows several peaks of an interesting compound with the retention time as shown in Figure 2(a). The mass spectra of interested compounds adsorbed on *Riccia* were identified by comparison with the NIST database. The interesting chemical constituent of substances adsorbed on *Riccia* with retention time 2.964–9.892 min and predominant fragment at m/z 156– m/z 278 were shown in Table 5. According to the result of the HS-GC-MS chromatogram and mass spectra, *Riccia* can be adsorbed by the particulate matter of several compounds related to air pollutants.

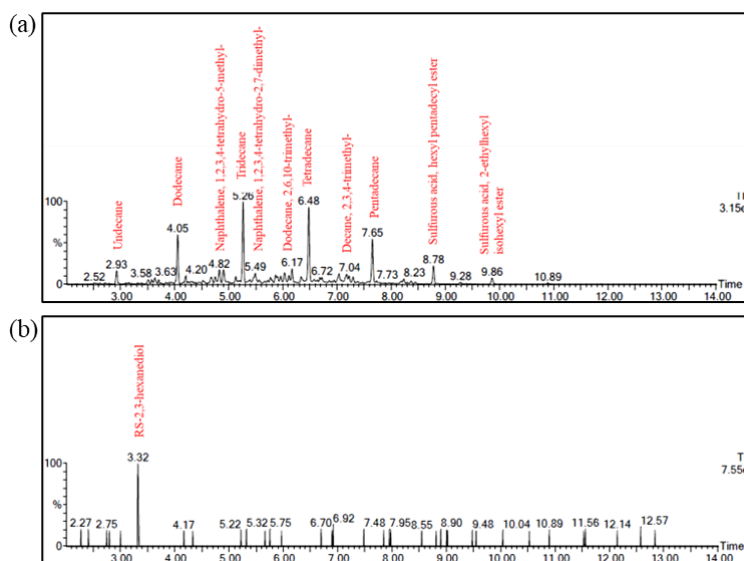


Figure 2. HS-GC-MS chromatogram (a) particulate matter treated (b) particulate matter untreated.

Table 5. The chemical constituent of substances adsorbed on *Riccia* compared to the NIST database.

| RT (min) | Compound name | m/z | CAS number | Structure |
|----------|--|-----|---------------|--|
| 2.964 | Undecane | 156 | 1120-21-4 | <chem>CCCCCCCCCCC</chem> |
| 3.670 | Butylbenzene | 134 | 104-51-8 | <chem>CCCCc1ccccc1</chem> |
| 4.099 | Dodecane | 170 | 112-40-3 | <chem>CCCCCCCCCCCCC</chem> |
| 4.244 | 2,-6dimethyl-Undecane | 184 | 17301-23-4 | <chem>CC(C)CCCC(C)CCCC</chem> |
| 4.710 | 2-methyl-1-octanol | 143 | 818-81-5 | <chem>CCCC(C)CCO</chem> |
| 4.865 | 1,2,3,4-tetrahydro-6-methyl- Naphthalene | 146 | 1680-51-9 | <chem>CC1=CC=C2CCCC2=C1</chem> |
| 5.310 | Tridecane | 184 | 629-50-5 | <chem>CCCCCCCCCCCCC</chem> |
| 6.210 | 2,6,10-trimethyl-Dodecane | 212 | 3891-98-3 | <chem>CC(C)CC(C)CC(C)CCCC</chem> |
| 6.515 | Tetradecane | 198 | 629-59-4 | <chem>CCCCCCCCCCCCC</chem> |
| 7.686 | Pentadecane | 212 | 629-62-9 | <chem>CCCCCCCCCCCCC</chem> |
| 8.817 | Sulfurous acid, hexyl octyl ester | 278 | Not available | <chem>CCCCCCCCOS(=O)(=O)OCCCCCCCC</chem> |
| 9.892 | Sulfurous acid, 2-ethyl hexyl hexyl isohexyl ester | 278 | Not available | <chem>CCCC(C)CCOS(=O)(=O)OCCCC(C)CC</chem> |

3.5. Metal analysis

Cd, Pb, and Na were determined using a Flame atomic absorption spectrophotometer (Perkin-

Elmer, PinAAcle 900F). The hollow cathode lamps for Cd, Pb, and Na were used as radiation sources and the fuel was air acetylene. All the standards and samples were run in triplicates. Metals concentrations of *Riccia* and its blank were determined using FAAS and the results obtained were shown in Table 6. *Riccia* shows the quantity of Cd, Pb, and Na 0.0044 ± 0.0069 mg/gDW, 0.0208 ± 0.0278 mg/gDW, and 0.9395 ± 0.1009 mg/gDW, respectively. The results suggest that *Riccia* can be adsorbed with some heavy metal in the environment. However, the quantity of analyte metal from particulate matter treated and untreated *Riccia* shows the result is not different.

Table 6. The concentration of metal analyte in plant samples.

| Metal | Plant samples | |
|-------------|---------------------|------------------------|
| | <i>Riccia</i> | Blank of <i>Riccia</i> |
| Cd (mg/gDW) | 0.0044 ± 0.0069 | 0.0048 ± 0.0019 |
| Pb (mg/gDW) | 0.0208 ± 0.0278 | 0.0320 ± 0.0464 |
| Na (mg/gDW) | 0.9395 ± 0.1009 | 0.9800 ± 0.2700 |

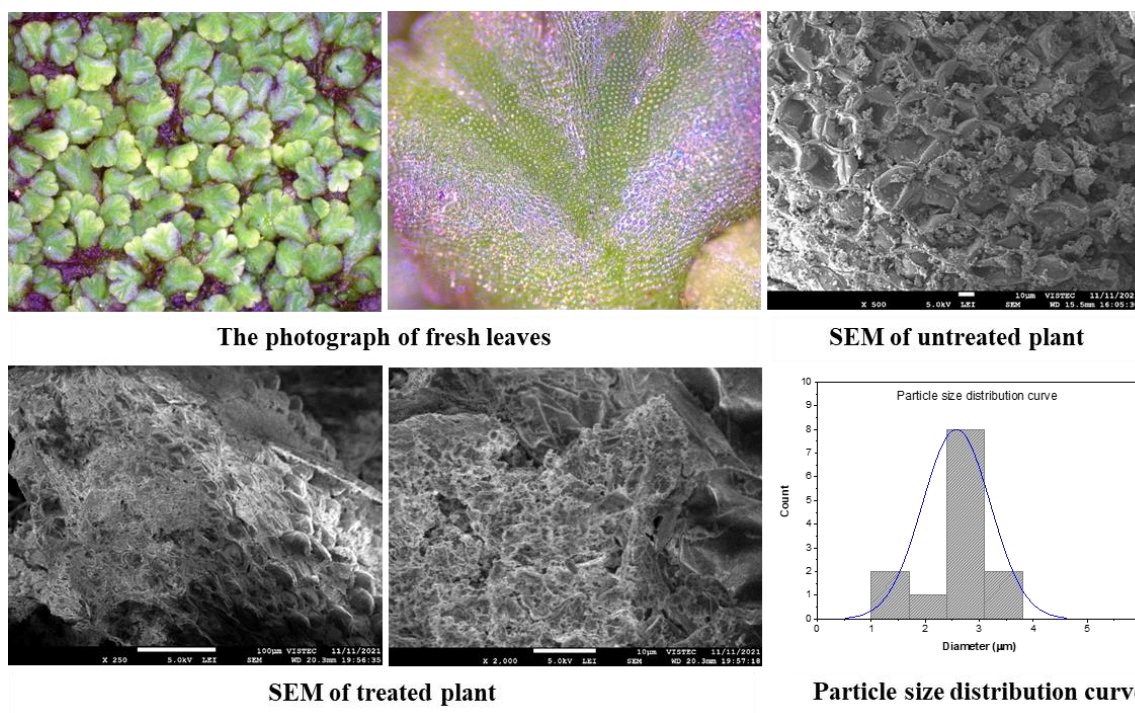


Figure 3. The photographs of *Riccia* show a portion of fleshy thalli (the upper left), a close-up of thallus showing oil bodies (the upper middle), SEM of the dorsal view of thalli before being treated showing globose-subglobose epidermal cells (the upper right), SEM photographs of thalli in cross-section after being treated (the lower left and middle) and the distribution curve showing the particle size covered on the thallus surface (the lower right). Scanning electron micrograph before deposited air pollutants at 500 \times magnification, SEM photograph of the particles deposited over the surface at 250 \times magnification and 2000 \times magnification.

3.6. Morphology of plant

The feature of *Riccia*, a non-vascular land plant, classified into the family Ricciaceae of Marchantiophyta, is distinctive in having oil bodies and non-sporogenous cells. It can be easily identified by a flat, dichotomously branched, ribbon-like, and fleshy thallus in the gametophytic stage as shown in Figure 3 (the upper left and the middle). Scanning electron micrographs of liverworts exhibited cells occupied by arbuscules in the main colonization zone within the thallus tissue which is a flattened mass of tissue. After air pollutants were deposited on plant samples in the gas form via wet deposition, the SEM image revealed that the particles covered the thallus surface. The particle size was obtained from a mean value of two values equivalent to the orthogonal axes. The final values of all particles were distributed by the size ranging from less than 1–4 μm .

4. Conclusions

In this study, the effectiveness of *Riccia* as a biofilter for adsorbed particulate matter in the urban ecosystem was investigated. Due to its morphology which is a complex thalloid, oil leaf, and non-sporogenous cells, and its ecology, which adsorbs the nutrients and water from the air through its outer surfaces [39,40], therefore *Riccia* was selected as a study plant as a biofilter of pollutants. The physical properties, physiological, and biological were measured to evaluate the particulate matter capture potential. The results revealed *Riccia* can be absorbed some minerals or trace elements through its surface via the stomata. Furthermore, *Riccia* can exist in unfavourable environmental conditions and adjust its tissue fluids to the new environment. Besides, *Riccia* was classified in a sensitive group with a lower air pollution tolerance index (APTI) value of 9.27 which is indicated that *Riccia* can be used as a biomonitoring plant for air pollution. According to the previous study, the ability to capture the elements of plants depending on their leaf properties [62] such as phyllotaxy, leaf shape, size and texture, presence or absence of hairs, stomatal frequency, stomatal density, surface roughness, and trichome length [63]. The biofiltration process consists of two major steps; are sorption and biodegradation in the removal of the contaminants from air or water. In the sorption step, there are two major mechanisms including adsorption by cuticle and uptake by opened stomata [64]. *Epipremnum aureum* was via stomata of plants and elected to use as a biofilter with the removal efficiencies of 85% for total suspended particles, 75.2% for PM_{2.5}, and 71.9% for PM₁₀ [57]. The use of *Tillandsia usneoides* as biofilter exhibited higher removal efficiency of 16.5% and 9.2% in PM_{2.5} from incense and A1 rigid, respectively. Moreover, *T. usneoides* with trichome structure exhibited larger removal efficiencies than without trichome, which indicates that the increase in the total effective surface was effective for the deposition of PM [58].

Herein, the removal efficiency of the particulate matter was determined and expressed to the adsorption efficiency. The alignment of the plant in the treatment box is three types, horizontal panels, zigzags panels, and vertical panels with four different velocities of 0.5, 1.0, 1.5, and 2.0 m/s. The highest efficiency values for PM₁, PM_{2.5}, and PM₁₀ were 31.4, 40.1, and 49.6, respectively, which belonged to the horizontal panel with a velocity of 2.0 m/s due to the high airflow velocity creating turbulence and generating transverse motion which enhances the rate of energy and momentum exchange increasing heat transfer and friction coefficient leading to gas-solid mass transfer between air pollutants and sample plants via stomata. The VOCs and PAHs were analyzed from the plants after being treated with air pollutants generated by diesel B7. The result revealed twelve compounds from

treated *Riccia* as compared to untreated *Riccia*, which indicate *Riccia* can be adsorbed with VOCs and PAHs. Consequently, metals such as Cd, Pb, and Na were determined and exhibited the analyte metal in treated *Riccia*, however, the quantity of analyte metal from treated and untreated *Riccia* is not significantly different. The morphology of *Riccia* shows a portion of fleshy thalli, oil bodies, globose-subglobose epidermal cells, and roughness surface which is characteristic of *Riccia*. Additionally, the treated *Riccia* shows the particulate matter cover on the thallus surface, and the particle sizes were in the range of 1–4 μm . These results indicate that the removal efficiency of particulate matter using *Riccia* is effective owing to this method being sustainable, easy-to-manage, and eco-friendly practices.

Due to peculiar morphological and physiological characteristics, mosses are very suitable adsorbents for a wide variety of pollutants (i.e., metals and metalloids, PAHs, radionuclides) and, when used as transplants in nylon bags, they allow easy monitoring potentially of any site, with a highly dense sampling network. Nevertheless, the technique uses moss-bag methods for the biomonitoring of air pollution but there are still limitations and less metal uptake occurs. The other variables (climate, bag size, shape, exposure time, and height) had low or no influence at all [65]. Innovation of this study used Computational Fluid Dynamics (CFD) as a modeling technique that can predict in terms of area and time. The research on airflow and indoor air circulation has been studied and applied [66,67]. CFDs can provide accurate information about flow distribution and concentrations in modeling domains, rather than only target areas for data collection [68,69]. Model boxes were constructed to study airflow data through 12 locations in the treatment box model, such as air velocity, flow characteristics, and air temperature distribution. Air in treatment box model 2 was circulated through every location. The airflow average that passed through 12 locations was similar throughout the treatment mode at all velocities of inlet air, airflow passed through all locations and contacted the surfaces of every panel. As a result, there was a high being absorbed by air pollution treatment by plants such as mosses and lichen to assess the concentration of heavy metal in the atmosphere [38]. In the future, possibility to apply *Riccia* as a biofilter of a large-scale urban site to detect emission sources and quantitative analysis of airborne persistent pollutants.

Acknowledgments

The authors would like to express their appreciation for the grant from the National Research Council of Thailand (NRCT) and Udon Thani Rajabhat University which all supported this paper. We would like to thank Prof. Vinich Promarak, the Smart Materials and Semiconductor Devices Laboratory, Vidyasirimedhi Institute of Science and Technology (VISTEC) for SEM analysis assistance. We also thank Assoc. Prof. Sahut Chantanaorrapint, PSU Herbarium, Division of Biological Science, Faculty of Science Prince of Songkla University for plant identification.

Conflict of interest

The authors declare no conflict of interest.

References

1. Sima V, Gheorghe IG, Subić J, et al. (2020) Influences of the Industry 4.0 Revolution on the human capital development and consumer behavior: A systematic review. *Sustainability* 12: 4035. <https://doi.org/10.3390/su12104035>
2. Bringezu S, Schütz H, Steger S, et al. (2004) International comparison of resource use and its relation to economic growth. *Ecol Econ* 51: 97–124. <https://doi.org/10.1016/j.ecolecon.2004.04.010>
3. Venables AJ (2016) Using natural resources for development: Why has it proven so difficult? *J Econ Perspect* 30: 161–184. <https://doi.org/10.1257/jep.30.1.161>
4. Almeida TAdN, Cruz L, Barata E, et al. (2017) Economic growth and environmental impacts: An analysis based on a composite index of environmental damage. *Ecol Indic* 76: 119–130. <https://doi.org/10.1016/j.ecolind.2016.12.028>
5. Schwarze P, Stilianakis N, Momas I, et al. (2005) Health effects of transport-related air pollution. <https://doi.org/10.1038/s12276-020-0403-3>
6. Schraufnagel DE (2020) The health effects of ultrafine particles. *Exp Mol Med* 52: 311–317. <https://doi.org/10.1038/s12276-020-0403-3>
7. Kwon HS, Ryu MH, Carlsten C (2020) Ultrafine particles: Unique physicochemical properties relevant to health and disease. *Exp Mol Med* 52: 318–328. <https://doi.org/10.1038/s12276-020-0405-1>
8. Moreno-Ríos AL, Tejeda-Benítez LP, Bustillo-Lecompte CF (2022) Sources, characteristics, toxicity, and control of ultrafine particles: An overview. *Geosci Front* 13: 101147. <https://doi.org/10.1016/j.gsf.2021.101147>
9. Li HL, Zheng Y, Yu Q, et al. (2022) Optimization for enhanced electrokinetic treatment of air pollution control residues using response surface methodology focusing on heavy metals leaching risk and extractability. *Process Saf Environ* 159: 534–546. <https://doi.org/10.1016/j.psep.2022.01.033>
10. Sawasdee V, Pisutpaisal N (2016) Simultaneous pollution treatment and electricity generation of tannery wastewater in air-cathode single chamber MFC. *Int J Hydrogen Energ* 41: 15632–15637. <https://doi.org/10.1016/j.ijhydene.2016.04.179>
11. Panahi Y, Mellatyar H, Farshbaf M, et al. (2018) Biotechnological applications of nanomaterials for air pollution and water/wastewater treatment. *Mater Today: Proc* 5: 15550–15558. <https://doi.org/10.1016/j.matpr.2018.04.162>
12. Bhatt P, Pandey SC, Joshi S, et al. (2022) Nanobioremediation: A sustainable approach for the removal of toxic pollutants from the environment. *J Hazard Mater* 427: 128033. <https://doi.org/10.1016/j.jhazmat.2021.128033>
13. Mohamed EF (2017) Nanotechnology: Future of environmental air pollution control. *Environ Manag Sust Dev* 6: 429–454. <https://doi.org/10.5296/emsd.v6i2.12047>
14. García-Mayagoitia S, Pérez-Hernández H, Medina-Pérez G, et al. (2020) Bio-nanomaterials in the air pollution treatment, In: *Nanomaterials for air remediation*, Amsterdam: Elsevier, 227–248.
15. Yadav KK, Singh JK, Gupta N, et al. (2017) A review of nanobioremediation technologies for environmental cleanup: A novel biological approach. *J Mater Environ Sci* 8: 740–757.

16. Singh BSM, Singh D, Dhal NK (2022) Enhanced phytoremediation strategy for sustainable management of heavy metals and radionuclides. *Case Stud Chem Environ Eng* 5: 100176. <https://doi.org/10.1016/j.cscee.2021.100176>
17. World Health Organization, WHO Collaborating Centre on Air Pollution Control, WHO Collaborating Centre on Clinical and Epidemiological Aspects of Air Pollution (1976) Selected methods of measuring air pollutants/prepared in cooperation with the WHO Collaborating Centre on Air Pollution Control, Office of Research and Development, U.S. Environmental Protection Agency, Washington, DC, USA and WHO Collaborating Centre on Clinical and Epidemiological Aspects of Air Pollution, Medical Research Council Air Pollution Unit, St. Bartholomew's Hospital Medical College, London, England. Available from: <https://apps.who.int/iris/handle/10665/37047>.
18. Language B, Piketh SJ, Burger RP (2016) Correcting respirable photometric particulate measurements using a gravimetric sampling method. *Clean Air J* 26: 10–14. <https://doi.org/10.17159/2410-972X/2016/v26n1a7>
19. Amaral S, de Carvalho J, Costa M, et al. (2015) An overview of particulate matter measurement instruments. *Atmosphere* 6: 1327–1345. <https://doi.org/10.3390/atmos6091327>
20. Smodiš B, Parr RM (1999) Biomonitoring of air pollution as exemplified by recent IAEA programs. *Biol Trace Elem Res* 71: 257–266. <https://doi.org/10.1007/BF02784211>
21. Costa C, Teixeira JP (2014) Biomonitoring, In: *Encyclopedia of toxicology*, 3 Eds., Oxford: Academic Press, 483–484. <https://doi.org/10.1016/B978-0-12-386454-3.01000-9>
22. Kousehlar M, Widom E (2019) Sources of metals in atmospheric particulate matter in Tehran, Iran: Tree bark biomonitoring. *Appl Geochem* 104: 71–82. <https://doi.org/10.1016/j.apgeochem.2019.03.018>
23. Gueguen F, Stille P, Lahd Geagea M, et al. (2012) Atmospheric pollution in an urban environment by tree bark biomonitoring-Part I: Trace element analysis. *Chemosphere* 86: 1013–1019. <https://doi.org/10.1016/j.chemosphere.2011.11.040>
24. Berlizov AN, Blum OB, Filby RH, et al. (2007) Testing applicability of black poplar (*Populus nigra* L.) bark to heavy metal air pollution monitoring in urban and industrial regions. *Sci Total Environ* 372: 693–706. <https://doi.org/10.1016/j.scitotenv.2006.10.029>
25. Zampieri MCT, Sarkis JES, Pestana RCB, et al. (2013) Characterization of *Tibouchina granulosa* (Desr.) Cong. (Melastomataceae) as a biomonitor of air pollution and quantification of particulate matter adsorbed by leaves. *Ecol Eng* 61: 316–327. <https://doi.org/10.1016/j.ecoleng.2013.09.050>
26. González CM, Casanovas SS, Pignata ML (1996) Biomonitoring of air pollutants from traffic and industries employing *Ramalina ecklonii* (Spreng.) Mey. and Flot. in Córdoba, Argentina. *Environl Pollut* 91: 269–277. [https://doi.org/10.1016/0269-7491\(95\)00076-3](https://doi.org/10.1016/0269-7491(95)00076-3)
27. Garty J, Garty-Spitz RL (2015) Lichens and particulate matter: Inter-relations and biomonitoring with lichens, In: *Recent advances in lichenology*, New Delhi: Springer, 47–85. https://doi.org/10.1007/978-81-322-2181-4_3
28. Massimi L, Castellani F, Protano C, et al. (2021) Lichen transplants for high spatial resolution biomonitoring of Persistent Organic Pollutants (POPs) in a multi-source polluted area of Central Italy. *Ecol Indic* 120: 106921. <https://doi.org/10.1016/j.ecolind.2020.106921>
29. Kousehlar M, Widom E (2020) Identifying the sources of air pollution in an urban-industrial setting by lichen biomonitoring-A multi-tracer approach. *Appl Geochem* 121: 104695. <https://doi.org/10.1016/j.apgeochem.2020.104695>

30. Thomas W (1986) Representativity of mosses as biomonitor organisms for the accumulation of environmental chemicals in plants and soils. *Ecotoxicol Environ Saf* 11: 339–346. [https://doi.org/10.1016/0147-6513\(86\)90106-5](https://doi.org/10.1016/0147-6513(86)90106-5)
31. Tak AA, Kakde UB (2017) Assessment of air pollution tolerance index of plants: A comparative study. *Int J Pharm Pharm Sci* 9: 83–89. <https://doi.org/10.22159/ijpps.2017v9i7.18447>
32. Isaac-Olive K, Solis C, Martinez-Carrillo MA, et al. (2012) *Tillandsia usneoides* L, a biomonitor in the determination of Ce, La and Sm by neutron activation analysis in an industrial corridor in Central Mexico. *Appl Radiat Isotopes* 70: 589–594. <https://doi.org/10.1016/j.apradiso.2012.01.007>
33. Techato K, Salaeh A, van Beem NC (2014) Use of Atmospheric Epiphyte *Tillandsia usneoides* (Bromeliaceae) as Biomonitor. *APCBEE Proc* 10: 49–53. <https://doi.org/10.1016/j.apcbee.2014.10.014>
34. Gallego-Cartagena E, Morillas H, Carrero JA, et al. (2021) Naturally growing grimmiaceae family mosses as passive biomonitors of heavy metals pollution in urban-industrial atmospheres from the Bilbao Metropolitan area. *Chemosphere* 263: 128190. <https://doi.org/10.1016/j.chemosphere.2020.128190>
35. Nikam J, Archer D, Nopsert C (2021) *Air quality in Thailand: Understanding the regulatory context*, Stockholm: Academic Press.
36. Boonpeng C, Sangiamdee D, Noikrad S, et al. (2020) Metal accumulation in lichens as a tool for assessing atmospheric contamination in a natural park. *Environ Nat Resour J* 18: 166–176. <https://doi.org/10.32526/enrj.18.2.2020.16>
37. Kayee P, Songphim W, Parkpein A (2015) Using Thai native moss as bio-adsorbent for contaminated heavy metal in air. *Proc-Soc Behav Sci* 197: 1037–1042. <https://doi.org/10.1016/j.sbspro.2015.07.312>
38. Meesang W, Baothong E, Poojeera S, et al. (2022) Model feasibility of air pollution treatment using plants as filter by computational fluid dynamic (CFD) analysis: A case study in laboratory. *Environ Asia* 15: 142–153. <http://doi.org/10.14456/ea.2022.13>
39. Cargill DC, Beckmann K, Seppelt R (2021) Taxonomic revision of *Riccia* (Ricciaceae, Marchantiophyta) in the monsoon tropics of the Northern Territory, Australia. *Aust Syst Bot* 34: 336–430. <https://doi.org/10.1071/sb20030>
40. Lee GE, Gradstein S (2021) *Guide to the liverworts and hornworts of Malaysia*, Tokyo: Hattori Botanical Laboratory.
41. Świsłowski P, Vergel K, Zinicovscaia I, et al. (2022) Mosses as a biomonitor to identify elements released into the air as a result of car workshop activities. *Ecol Indic* 138: 108849. <https://doi.org/10.1016/j.ecolind.2022.108849>
42. Kosior G, Samecka-Cymerman A, Brudzinska-Kosior A (2018) Transplanted Moss *Hylocomium splendens* as a Bbioaccumulator of trace elements from different categories of sampling sites in the Upper Silesia area (SW Poland): Bulk and dry deposition impact. *Bull Environ Contam Toxicol* 101: 479–485. <https://doi.org/10.1007/s00128-018-2429-y>
43. Capozzi F, Adamo P, Spagnuolo V, et al. (2021) Field comparison between moss and lichen PAHs uptake abilities based on deposition fluxes and diagnostic ratios. *Ecol Indic* 120: 106954. <https://doi.org/10.1016/j.ecolind.2020.106954>
44. Read DJ, Edwards D, Read DJ, et al. (2000) Symbiotic fungal associations in ‘lower’ land plants. *Phil Trans R Soc Lond B* 355: 815–831. <https://doi.org/10.1098/rstb.2000.0617>

45. Ghafari S, Kaviani B, Sedaghatoor S, et al. (2020) Assessment of air pollution tolerance index (APTI) for some ornamental woody species in green space of humid temperate region (Rasht, Iran). *Environ Dev Sust* 23: 1579–1600. <https://doi.org/10.1007/s10668-020-00640-1>
46. Ferella F, Zueva S, Innocenzi V, et al. (2018) New scrubber for air purification: Abatement of particulate matter and treatment of the resulting wastewater. *Int J Environ Sci Technol* 16: 1677–1690. <https://doi.org/10.1007/s13762-018-1826-4>
47. Vianna NA, DG, Brandao F, de Barros RP, et al. (2011) Assessment of heavy metals in the particulate matter of two Brazilian metropolitan areas by using *Tillandsia usneoides* as atmospheric biomonitor. *Environ Sci Pollut Res Int* 18: 416–427. <https://doi.org/10.1007/s11356-010-0387-y>
48. Che YH, Yao TT, Wang HR, et al. (2022) Potassium ion regulates hormone, Ca²⁺ and H₂O₂ signal transduction and antioxidant activities to improve salt stress resistance in tobacco. *Plant Physiol Biochem* 186: 40–51. <https://doi.org/https://doi.org/10.1016/j.plaphy.2022.06.027>
49. Nwajinka CO, Okonjo EO, Amaefule DO, et al. (2020) Effects of microwave power and slice thickness on fiber and ash contents of dried sweet potato (*Ipomoea batata*). *NIJOTECH* 39: 932–941. <https://doi.org/10.4314/njt.v39i3.36>
50. Wherry ET, Buchanan R (1926) Composition of the ash of Spanish-moss. *Ecology* 7: 303–306. <https://doi.org/10.2307/1929312>
51. Gortner RA, Hoffman WF (1992) Determination of moisture content of expressed plant tissue fluids. *Bot Gaz* 74: 308–313.
52. Ahmad S, Amin MN, Mosaddik MA (2002) Studies on moisture content, biomass yield (crude plant extract) and alkaloid estimation of *in vitro* and field grown plants of *Rauvolfia serpentina*. *Pak J Biol Sci* 5: 416–418.
53. Yoshikawa K, Overduin PP, Harden JW (2004) Moisture content measurements of moss (*Sphagnum* spp.) using commercial sensors. *Permafrost Periglacial Processes* 15: 309–318. <https://doi.org/10.1002/ppp.505>
54. Kim DM, Zhang HR, Zhou HY, et al. (2015) Highly sensitive image-derived indices of water-stressed plants using hyperspectral imaging in SWIR and histogram analysis. *Sci Rep* 5: 15919. <https://doi.org/10.1038/srep15919>
55. Krishnaveni M, Chandrasekar R, Amsavalli L, et al. (2013) Air pollution tolerance index of plants at Perumalmalai Hills, Salem, Tamil Nadu, India. *Int J Pharm Sci Rev Res* 20: 234–239.
56. Wang HX, Shi H, Li YY (2011) Leaf dust capturing capacity of urban greening plant species in relation to leaf micromorphology. *2011 International Symposium on Water Resource and Environmental Protection*, 2198–2201.
57. Hamontree C, Ibrahim IZ, Chong W-T, et al. (2018) The design of the botanical indoor air biofilter system for the atmospheric particle removal. *MATEC Web Conf* 192: 02035. <https://doi.org/10.1051/mateconf/201819202035>
58. Kim JJ, Park J, Jung SY, et al. (2020) Effect of trichome structure of *Tillandsia usneoides* on deposition of particulate matter under flow conditions. *J Hazard Mater* 393: 122401. <https://doi.org/10.1016/j.jhazmat.2020.122401>
59. Shen L, Zhang X, Yue DKP, et al. (2003) Turbulent flow over a flexible wall undergoing a streamwise travelling wave motion. *J Fluid Mech* 484: 197–221. <https://doi.org/10.1017/s0022112003004294>

60. Gul A, Tezcan Un U (2022) Effect of temperature and gas flow rate on CO₂ capture. *Eur J Sust Dev Res* 6: em0181. <https://doi.org/10.21601/ejosdr/11727>
61. Saysroy A, Eiamsa-ard S (2017) Enhancing convective heat transfer in laminar and turbulent flow regions using multi-channel twisted tape inserts. *Int J Therm Sci* 121: 55–74. <https://doi.org/10.1016/j.ijthermalsci.2017.07.002>
62. Choi YK, Song HJ, Jo JW, et al. (2021) Morphological and chemical evaluations of leaf surface on particulate matter_{2.5} (PM_{2.5}) removal in a botanical plant-based biofilter system. *Plants* 10: 2761. <https://doi.org/10.3390/plants10122761>
63. Wang YC, Chen B (2021) Dust capturing capacity of woody plants in clean air zones throughout Taiwan. *Atmosphere* 12: 696. <https://doi.org/10.3390/atmos12060696>
64. Fernandez V, Gil-Pelegrin E, Eichert T (2021) Foliar water and solute absorption: An update. *Plant J* 105: 870–883. <https://doi.org/10.1111/tpj.15090>
65. Palma AD (2016) Mosses for monitoring air pollution: Towards the standardization of moss-bag technique and the set-up of a new biomaterial, PhD thesis, University of Naples Federico II.
66. Usman F, Bakar ARA, Mohamed Nazri F (2020) Thermal comfort study using CFD analysis in residential house with mechanical ventilation system, In: *Proceedings of AICCE'19*, Cham: Springer.
67. Liu J, Heidarinejad M, Pitchurov G, et al. (2018) An extensive comparison of modified zero-equation, standard k- ϵ , and LES models in predicting urban airflow. *Sust Cities Soc* 40: 28–43. <https://doi.org/10.1016/j.scs.2018.03.010>
68. Muhsin F, Yusoff WFM, Mohamed MF et al. (2017) CFD modeling of natural ventilation in a void connected to the living units of multi-storey housing for thermal comfort. *Energ Build* 144: 1–16. <https://doi.org/10.1016/j.enbuild.2017.03.035>
69. Zhang Y, Yu WX, Li YL, et al. (2021) Comparative research on the air pollutant prevention and thermal comfort for different types of ventilation. *Indoor Built Environ* 30: 1092–1105. <https://doi.org/10.1177/1420326x20925521>



AIMS Press

© 2023 the Author(s), licensee AIMS Press. This is an open access article distributed under the terms of the Creative Commons Attribution License (<http://creativecommons.org/licenses/by/4.0>)